PHYSICAL REVIEW A, VOLUME 61, 031403(R)

Compression of cold atoms to very high densities in a rotating-beam blue-detuned optical trap

N. Friedman, L. Khaykovich, R. Ozeri, and N. Davidson
Department of Physics of Complex Systems, Weizmann Institute of Science, Rehovot 76100, Israel

(Received 21 July 1999; published 3 February 2000)

We propose and demonstrate a scheme for a blue-detuned optical dipole trap for cold atoms which consists of a single, rapidly rotating laser beam. We characterize a parameter range in which the optical potential can be accurately described by a quasistatic time-averaged potential. The trap is loaded with $>10^6$ Rb atoms, and is then compressed adiabatically by a factor of 350 to a final density of 5×10^{13} cm^{-3}. A$\sim$4 times adiabatic increase in the peak phase-space density of the trapped atoms is obtained due to the change in the shape of the trap potential. The two-body elastic and inelastic collision rates of atoms in the compressed trap are determined.

PACS number(s): 32.80.Pj, 42.50.Vk, 39.90.+d

Obtaining high atomic phase-space densities in optical dipole traps has attained much interest lately, and has led to demonstrations of new laser-cooling schemes at high densities in red-detuned traps [1–3]. Since a large detuning of the trapping light from an atomic resonance is required to supress spontaneous emission, the depth of the optical potential and hence the density and number of atoms in these traps are limited. Blue-detuned dipole traps, where repulsive light forces confine atoms mostly in the dark, provide weak perturbations of atomic coherences combined with a steep potential [4]. This enables observation of much longer coherence times, and may lead to higher densities than in comparable red-detuned traps. Unfortunately, the complexity of forming blue-detuned traps limits their wide use. Hence single-beam blue-detuned traps are of a great interest thanks to their possible flexibility in manipulating the trapping potential size and shape [5].

In this Rapid Communication we present a configuration of a single-beam blue-detuned optical trap, based on a rapidly rotating laser beam that traps atoms in a dark volume completely surrounded by light. Since the trap is realized with a single laser beam, large dynamical changes of the potential size and shape were readily obtained. A large initial volume provided an efficient loading into the trap, and an adiabatic decrease of the trap size yielded a dramatic increase in the potential depth and in the atomic density. This resulted in a very dense atomic cloud with a relatively large number of atoms. Recently, a similar dynamic compression was reported in a microscopic magnetic trap, though with a moderate number of atoms [6].

Rotating laser beams were used as optical tweezers to trap reflective particles [7], and also to trap atoms in a two-dimensional trap [8]. However, the very low rotation frequencies (<1kHz) in those configurations made them unsuitable for trapping high-density atomic samples.

Our rotating beam optical trap (ROBOT) is composed of a linearly polarized, tightly focused Gaussian laser beam ($1/e^2$ radius of $w_0=16$ μm), which is rapidly (up to 400 kHz) rotating using two perpendicular acousto-optic scanners (AOS's) [9]. When the radius of rotation, r, is larger then w_0, a dark volume surrounded by light is obtained, as seen in Fig. 1. If the rotation frequency is high enough, the optical dipole potential can be approximated as a time-averaged quasistatic potential. In the beam propagation direction, the atoms are trapped by the divergence of the focused laser beam. The two lowest points in the (time-averaged) potential barrier of the trap are located on the optical axis [the center of the cross section in Fig. 1(c)]. In our trap, with a laser power of 200 mW, a detuning of $\delta=1.5$ nm above the D_2 line ($\lambda=780.2$ nm) of ^{85}Rb, and $r=100$ μm, this minimal potential height is 22 μK, and scales approximately as r^{-2}. These values for the laser power and detuning are assumed throughout this paper unless stated otherwise. Stable trapping of atoms in the ROBOT was obtained for a detuning range $\delta=0.1$–10 nm, and for a rotation-radius range $r=24-105$ μm ($r/w_0=1.5$–6.5).

The ROBOT was loaded from a compressed ^{85}Rb magneto-optical trap (MOT), described elsewhere [10]. Briefly, 700 ms of loading, 47 ms of compression, and 3 ms of polarization gradient cooling produced a cloud of $\sim3\times10^8$ atoms, with a temperature of 9 μK and a peak density of 1.5×10^{11} cm^{-3} . After all the laser beams were shut off (except for the rotating trapping beam which was overlapping the center of the MOT), a few million atoms were typically loaded into the trap, with temperatures and densities comparable to those of the MOT. The number of trapped atoms and the size of the trap were measured using fluorescence and absorption imaging. The fluorescence imaging was induced by a 100-μs strong laser pulse, resonant with the $5S_{1/2},F_g=3\rightarrow5P_{3/2},F_e=4$ transition. For the absorption imaging, a 20-μs pulse of a weak laser beam was applied from the transverse direction, and the trap shadow was imaged on a charge-coupled-device camera, with a resolution of $\sigma_{res}\simeq3$ μm. Temperature was measured using images obtained after ballistic expansion.

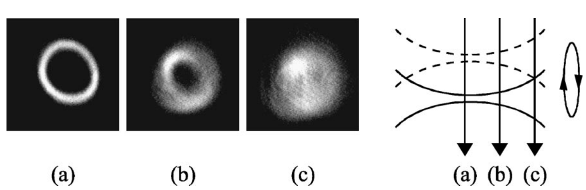

FIG. 1. Measured cross sections of the time-averaged intensity in three positions along the ROBOT, for a radius of rotation $r=100$ μm, together with a schematic drawing of the rotating laser beam.

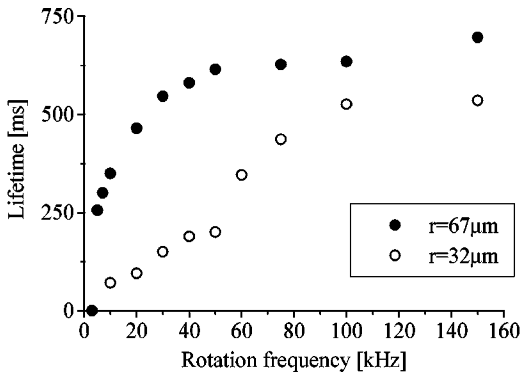

FIG. 2. Lifetime of the trapped atoms as a function of the rotation frequency of the trapping beam, for two trap radii.

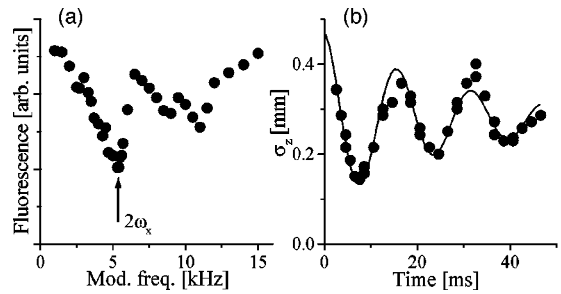

FIG. 3. Measurement of the oscillation frequencies of the ROBOT for $r=27$ μm. (a) Radial: fluorescence from the remaining atoms after 500 ms of 4% modulation of the potential depth, as a function of the modulation frequency. (b) Axial: size of the atomic cloud as a function of time after a sudden decrease in the rotation radius. The solid line is an exponentially decaying sine wave fit to the data.

We studied the stability of the trap by measuring the lifetime of the trapped atoms as a function of the rotation frequency, f_{rot}, of the trapping beam. For low atomic densities the trap lifetime was always well fitted by an exponential decay. The measured 1/e lifetimes are shown in Fig. 2, for two rotation radii. For $r=67$ μm, the trap became stable for $f_{rot}\gtrsim 20$ kHz, where the lifetime is $\sim$600ms, limited by collisions with hot background atoms. For $r=32$ μm, stable trapping was achieved only for $f_{rot}\gtrsim 60$ kHz. This is expected, since the oscillation frequency of the trapped atoms is higher in the smaller trap. The rest of the experiment was performed with $f_{rot}=100$ kHz, where the trap was stable over the whole radius range.

Next we characterized the time-averaged trapping potential by precisely measuring the oscillation frequencies of the trapped atoms in both the radial and axial directions. These measurements were done for $r/w_0<2$, where the time-averaged potential is approximately harmonic at its bottom. For $r=27$ μm a radial oscillation frequency of $\omega_x=2\pi \times 2680$ Hz was measured using a parametric excitation technique [11], as seen in Fig. 3(a). This value is in excellent agreement with values calculated either for the time-averaged potential or using a Monte Carlo (MC) simulation that included the full time dependence of the potential, which both gave $\omega_x=2\pi\times 2690$ Hz. This measurement was repeated for different trap radii, and a similar agreement with the calculations was obtained.

The axial oscillation frequency was measured by observing the oscillations in the size of the trapped atomic cloud after a sudden compression of the potential. The trap radius was decreased from $r_{initial}=100$ μm to $r_{final}=27$ μm in 1 ms, and the size of the atomic cloud along the trap axis was measured at different times after the compression. The results, which are presented in Fig. 3(b), show a breathing mode oscillation of the atoms in the final potential at twice the axial oscillation frequency $\omega_z= 2\pi\times 32$ Hz. Again, this value is in good agreement with our calculations, which both give $\omega_z=2\pi\times 29$ Hz. The precise characterization of the trapping potential served two purposes. First, it confirmed the validity of the time-averaged potential approximation in the limit of high rotation frequency. Second, it was used to verify the density of the trapped atoms when their radial size was comparable to the resolution of our imaging system.

To increase the density of the atomic sample adiabatically, the trap was slowly compressed from $r_{initial}$ to r_{final} in 150 ms. The number of trapped atoms was $N=1.2\times 10^6$, and no atoms were lost from the trap due to the compression. We verified that the compression is indeed adiabatic by observing that the cloud size after the compression did not oscillate by $>5\%$. The compressed atomic cloud had a nearly Gaussian density distribution with a measured rms axial size of $\sigma_z=300$ μm, and temperatures of $T_z=48$ μK in the axial direction and $T_x=124$ μK in the radial direction. Since the compression time is much longer than the radial oscillation time, the radial size σ_x can be deduced from the measured temperature and oscillation frequency, $\sigma_x=v_x/\omega_x=6.6$ μm, where v_x is the measured rms transverse velocity of the atoms. This size is in agreement with the size measured using the absorption imaging system ($\sigma_x=8.8$ μm), considering its resolution.

A further increase in the density was achieved by optically cooling the atomic sample. To prevent loss of atoms due to light assisted collisions [12] a short (1.5 ms) cooling pulse was applied. The lowest final temperatures, of $T_z=28$ μK and $T_x=41$ μK, were obtained when the cooling pulse was applied at $r=44$ μm with a detuning of -75 MHz from the $F_g=3\rightarrow F_e=4$ line [13]. An optimal timing for the cooling pulse is expected. When the cooling was applied in the early part of the compression ($r>44$ μm), the atoms were cooled back to their initial temperature but were heated during the remaining part of the compression. On the other hand, when the pulse was applied toward the end of the compression ($r<44$ μm), the density was already too high and optical cooling failed [14].

From the measured temperatures and oscillation frequencies we calculate the peak atomic density as $n_{\max}=N\omega_x^2\omega_z/(2\pi)^{3/2}v_x^2v_z=2\times 10^{13}$ cm^{-3} in the compressed trap with the cooling pulse applied, with an estimated uncertainty of a factor of 2. This represents a compression by a factor of 130 and a 16-fold increase in the peak phase-space density compared to the initial conditions.

Measurements of the decay of the number of trapped atoms indicate that two-body collision losses are becoming

RAPID COMMUNICATIONS

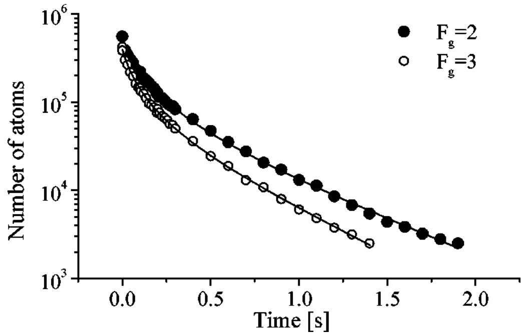

FIG. 4. Decay of the number of trapped atoms after the adiabatic compression, for the two hyperfine ground states. The solid lines are fits according to Eq. (1).

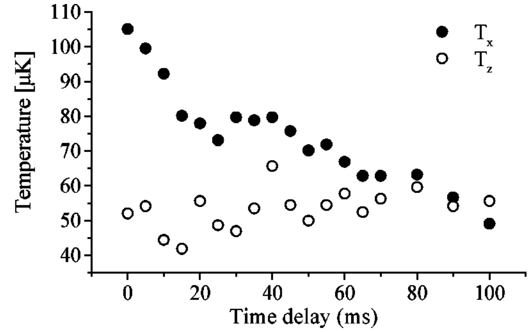

FIG. 5. Evolution of the radial and axial temperatures of the trapped atoms after the adiabatic compression.

important at the high densities obtained in the compressed trap. As seen in Fig. 4, the measured decay curves for atoms in either $F_g=3$ or $F_g=2$ [15] are well fitted by the solution of the rate equation,

$$dN/dt=-\alpha N-\beta\int n^2 dV=-\alpha N-\frac{1}{2.8}\frac{\beta N^2}{V}, \qquad (1)$$

where a three-dimensional Gaussian density distribution with a constant volume, $V=(2\pi)^{3/2}\sigma_x\sigma_y\sigma_z$, is assumed. The two-body collision loss coefficients found from that fit are $\beta_{F_g=3}=2.0\times10^{-11}$ cm^3/s and $\beta_{F_g=2}=1.2\times10^{-11}$ cm^3/s [16]. We believe that the loss from $F_g=2$ is caused by light-assisted collisions, where two colliding atoms come to resonance with the trap laser which excites them to a repulsive molecular potential curve, previously seen only for much smaller laser detunings [17]. The larger two-body collision loss from $F_g=3$ is due to hyperfine exchange collisions, given by $\beta_{hf}=\beta_{F_g=3}-\beta_{F_g=2}=0.8\pm0.6\times10^{-11}$ cm^3/s (assuming identical light-assisted loss for $F_g=2$ and 3). This value is consistent with previous measurements of $\beta_{hf}\sim1\times10^{-11}$ cm^3/s [18].

Another consequence of the high density in the compressed trap is high elastic collision rate. Immediately after the compression, the temperatures in the radial and axial directions are different due to the much larger compression in the radial direction. The temperature difference between the two axes then decays with a rate of ~30 s^{-1}, as seen from Fig. 5. Note that the initial elastic collision rate is even higher, since the temperature equalization rate is comparable to the density decay rate just after the compression. Of course, temperature equalization begins already at the final stage of the compression, when densities are sufficiently high. This is seen by the fact that the measured temperature at the end of the compression is lower in the radial direction and higher in the axial direction as compared to our MC simulations, which do not include elastic collisions [22].

We measured the spin relaxation time τ_{SR} of the trapped atoms by investigating spontaneous Raman scattering between the two ground-state hyperfine levels caused by the trapping laser [19,5]. For the largest trap we studied, with $r=100$ μm, we measured $\tau_{SR}=380\pm20$ ms. Using the analysis described in Ref. [5], the total photon scattering rate in this case is found to be $\gamma_s=7$ s^{-1}. For the compressed trap we similarly measured $\gamma_s=156$ s^{-1}. The 22-fold increase in the scattering rate is partly due to $\sim$10-fold increase in the kinetic energy of the trapped atoms, and partly due to the change in the shape of the trap potential from nearly boxlike to harmonic.

Finally, to obtain even stronger compression and to further increase the final atomic density, we decreased the detuning of the trapping laser to 0.5 nm, and decreased the final trap radius to $r=24$ μm. The resulting potential is $\times25$ higher than the initial, uncompressed potential. The calculated oscillation frequencies in this trap are $\omega_x=2\pi\times5800$ Hz and $\omega_z=2\pi\times60$ Hz. This trap could be loaded with a larger number of atoms, $N=3.5\times10^6$, thanks to its larger depth. The final temperatures after the compression were $T_z=108$ μK and $T_x=207$ μK, and the final size of the atomic cloud along the trap axis was $\sigma_z=250$ μm. Using the measured temperatures and size and the calculated ω_x, the peak density is determined as $n\sim5\times10^{13}$ cm^{-3}, which represents an adiabatic compression of $\times350$.

The peak phase-space density of this compressed state was 4.4 times higher than that of the initial, uncompressed trap. We attribute this increase to the change in the shape of the potential, from boxlike to harmonic [20]. Specifically, the initial (time-averaged) trapping potential of the ROBOT is well approximated as $U(x,y,z)=a_x x^{n_x}+a_y y^{n_y}+a_z z^{n_z}$, with $n_x=n_y=28$ and $n_z=6$ (for the initial temperature of the atoms), whereas the final, compressed potential is nearly harmonic in all dimensions $(n_x=n_y=n_z=2)$. The expected increase in peak phase-space density is [20] $\exp(\gamma_{final}-\gamma_{initial})=3.5$, where $\gamma=(n_x^{-1}+n_y^{-1}+n_z^{-1})$, and is in good agreement with our measurement.

To conclude, we demonstrated a dark optical trap for cold atoms, based on a single rapidly rotating laser beam. We verified experimentally that for a high rotation frequency of the trapping beam, the trapped atoms accurately respond to a time-averaged effective optical potential. By changing the trap size in real time, the trapping potential was increased by a factor of 25 without changing the trapping laser power, which resulted in a compression of the trapped atomic sample by a factor of 350, to a very high density. With a fivefold increase in the laser power, a trap with $r/\omega_0=20$, and changing δ from 0.5 to 10 nm during the compression, we estimate that $\sim 10^8$ atoms can be trapped, with a density of 10^{14} cm^{-3} and a total photon scattering rate of 3 s^{-1}.

Due to the high elastic collision rate and the excellent control over the trapping potential, this scheme can be a promising starting point for evaporative cooling inside an optical trap, to achieve quantum degeneracy. The excellent control over the trapping potential can be used to induce evaporation without decreasing the spring constant, by lowering the potential only in a specific region of the trap. A ROBOT with high r/ω_0 ratio and large δ seems most suitable for use in a search for a permanent electric-dipole moment, thanks to the reduced interaction of atoms with the trapping light and the precise control of the laser polarization which is possible in a single-beam setup [21]. Another possible application may be the investigation of chaotic atomic motion in a ROBOT with a noncircular cross section. Finally, the ROBOT can also be used to trap atoms with a red-detuned laser, where the laser will rotate the trapped atoms such that cold atomic samples with very large and controlled angular momentum can be created.

The authors would like to thank D. J. Heinzen for helpful discussion. This work was supported in part by the Israel Science Foundation. N. F. acknowledges support from the Israel Ministry of Science.

[1] D. Borion *et al.*, Phys. Rev. A **57**, R4106 (1998).
[2] V. Vuletic, C. Chin, A. J. Kerman, and S. Chu, Phys. Rev. Lett. **81**, 5768 (1998).
[3] M. T. DePue, C. McCormick, S. L. Winoto, S. Oliver, and D. S. Weiss, Phys. Rev. Lett. **82**, 2262 (1999).
[4] N. Davidson, H.J. Lee, C.S. Adams, M. Kasevich, and S. Chu, Phys. Rev. Lett. **74**, 1311 (1995).
[5] R. Ozeri, L. Khaykovich, and N. Davidson, Phys. Rev. A **59**, R1750 (1999).
[6] V. Vuletic, T. Fischer, M. Praeger, T. W. Hansch, and C. Zimmermann, Phys. Rev. Lett. **80**, 1634 (1998).
[7] K. Sasaki, M. Koshioka, H. Misawa, N. Kitamura, and H. Masuhara, Appl. Phys. Lett. **60**, 807 (1992).
[8] N. P. Bigelow (unpublished).
[9] A circular scan was produced by modulating the radio frequency of the two AOS's with a $\pi/2$ phase shift between the modulating signals. The radius of rotation was determined by the modulation amplitude.
[10] L. Khaykovich and N. Davidson, J. Opt. Soc. Am. B **16**, 702 (1999).
[11] S. Friebel, C. D'Andrea, J. Walz, M. Weitz, and T. W. Hansch, Phys. Rev. A **57**, R20 (1998).
[12] S. L. Winoto, M. T. DePue, N. E. Bramall, and D. S. Weiss, Phys. Rev. A **59**, R19 (1999).
[13] The temperatures of the atoms at this point were reduced from 17 μK (53 μK) to 10 μK (16 μK) in the axial (radial) direction.
[14] With a very small number of atoms we were able to cool the atoms back to their initial temperature even in a compressed trap.
[15] Since photons scattered from the trapping laser equalize the populations of the two hyperfine levels, a repumping (pumping) laser, resonant with the $F_g=2\rightarrow F_e=2$ ($F_g=3\rightarrow F_e=3$) transition, was applied to maintain a $>95\%$ population in the $F_g=3$ ($F_g=2$) state. However, similar decay rates were also obtained with no repumping and pumping lasers.
[16] To verify that the nonexponential loss is not caused by the compression process, we repeated it with a very small number of atoms, and found a purely exponential decay after compression.
[17] S. Bali, D. Hoffmann, and T. Walker, Europhys. Lett. **27**, 273 (1994).
[18] C. D. Wallace *et al.*, Phys. Rev. Lett. **69**, 897 (1992); S. D. Gensemer *et al.*, Phys. Rev. A **56**, 4055 (1997).
[19] R. A. Cline, J. D. Miller, M. R. Matthews, and D. J. Heinzen, Opt. Lett. **19**, 207 (1994).
[20] P. W. H. Pinkse *et al.*, Phys. Rev. Lett. **78**, 990 (1997).
[21] M. V. Romalis and E. N. Fortson, Phys. Rev. A **59**, 4547 (1999).
[22] Temperature measurements at lower densities and results of the MC simulations did not reveal temperature equalization, which verifies that equalization is caused by elastic collisions and not by the unharmonicity of the potential.